Bioorganic & Medicinal Chemistry Letters 19 (2009) 5387–5391

Contents lists available at ScienceDirect

Bioorganic & Medicinal Chemistry Letters

journal homepage: www.elsevier.com/locate/bmcl

Molecular modeling studies to predict the possible binding modes of endomorphin analogs in μ opioid receptor

Xin Liu [a], Ming Kai [a], Lian Jin [a], Rui Wang [a,b,*]

[a] Institute of Biochemistry and Molecular Biology, School of Life Sciences, State Key Laboratory of Applied Organic Chemistry, Lanzhou University, 222 Tianshui South Road, Lanzhou 730000, PR China
[b] State Key Laboratory of Chinese Medicine and Molecular Pharmacology, Department of Applied Biology and Chemical Technology, The Hong Kong Polytechnic University, Kowloon, Hong Kong, China

ARTICLE INFO

Article history:
Received 1 June 2009
Revised 9 July 2009
Accepted 25 July 2009
Available online 30 July 2009

Keywords:
Endomorphin analogs
Molecular docking
Molecular dynamics simulation
μ Opioid receptor

ABSTRACT

The molecular docking of a series of endomorphin analog with the μ opioid receptor was performed. The successive molecular dynamics of several proposed ligand–receptor complexes inserted into the phospholipid bilayer were carried out to optimize the complex and explore the conformational changes. Meaningful differences of their binding modes were detected and the involvement of some essential residues in ligand binding was also identified. Our proposed ligand–receptor model is in good agreement with previous site-directed mutagenesis experiments.

The three opioid receptors (μ, δ and κ) belong to the G-protein coupled receptors (GPCRs), which are characterized structurally with a core of seven helical transmembrane domains connected by three extracellular and intracellular loops.[1] These receptors are extremely important clinical target in the treatment of pain and additionally have profound effects on the neuroendocrine system immune response.[2] The μ opioid receptor (MOR) is proven to be the major target of analgesics,[2] because of the particular physiological characteristics of this receptor, development of the synthetic MOR-specific ligand is of great importance.

The endogenous peptide ligands for MOR, endomorphin-1 (Tyr-Pro-Trp-Phe-NH2, **EM1**), and endomorphin-2 (Tyr-Pro-Phe-Phe-NH2, **EM2**) were discovered by Zadina et al. in 1997.[3] These EMs exhibited the highest affinity for MOR receptor and extraordinarily high selectivity relative to delta-opioid and kappa-opioid receptor systems of all known opioid substances. These tetrapeptides have a strong antinociceptive effect on acute pain, similar to that of morphine. They are also more effective than the majority of the opioid peptides against neuropathic pain even at low doses, opening the possibility of using the two peptides as drugs.[4]

According to the 'message-address' concept, it is possible to consider that Tyr-Pro-Trp/Phe and Phe-NH2 correspond to the message and address domains, respectively.[5,6] These two domains of EMs play an important role in ligand recognition and binding. Recently, we have reported the binding affinities and bioactivities of a series of EM analogs with modifications related to the 'address' domain, and some of these analogs show good affinities and agonist behaviour.[7] Since EMs are regarded as important model peptides to determine the structure–activity relationship against their receptors, elucidating the binding mode for their action is crucial for further improvements of their structures.

In the present work, a representative series of EM analogs we have synthesized recently,[7] Table 1 and Figure 1, are flexibly docked to a model of the human MOR. Additionally, it seems to be possible to obtain more accurate docked complex model using molecular dynamics simulations in membrane environment. The goal was to evaluate the binding orientations, and conformations

Table 1
Opioid receptor binding affinities and in vitro pharmacological activity of EMs and EM analogs[a]

Peptides no.	Sequence	K_i (nM)	Potency
EM1	Tyr-Pro-Trp-Phe-NH2	4.55 (±0.16)	0.26
EM2	Tyr-Pro-Phe-Phe-NH2	8.23 (±0.48)	0.37
1	Tyr-Pro-Trp-D-Val-Bn	2.32 (±0.15)	0.70
2	Tyr-Pro-Phe-D-Val-Bn	4.97 (±1.24)	0.56
3	Tyr-Pro-Trp-D-Ala-Bn	4.56 (±0.84)	0.15
4	Tyr-Pro-Phe-D-Ala-Bn	8.67 (±1.27)	0.81
5	Tyr-Pro-Trp-Gly-Bn	56.23 (±7.0)	17.7
6	Tyr-Pro-Phe-Ala-Bn	122 (±17)	0.69

[a] Values are cited from our group's previous report.[7]

* Corresponding author. Fax: +86 931 8911255.
E-mail address: wangrui@lzu.edu.cn (R. Wang).

0960-894X/$ - see front matter © 2009 Elsevier Ltd. All rights reserved.
doi:10.1016/j.bmcl.2009.07.121

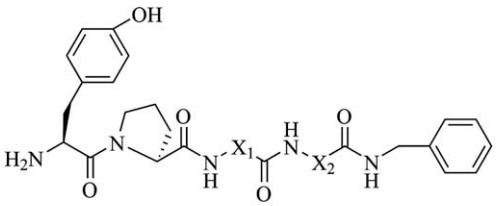

1. X_1=Trp, X_2=D-Val 2. X_1=Phe, X_2=D-Val

3. X_1=Trp, X_2=D-Ala 4. X_1=Phe, X_2=D-Ala

5. X_1=Trp, X_2=L-Gly 6. X_1=Phe, X_2=L-Ala

Figure 1. Schematic diagram of endomorphin analogs investigated in this study.

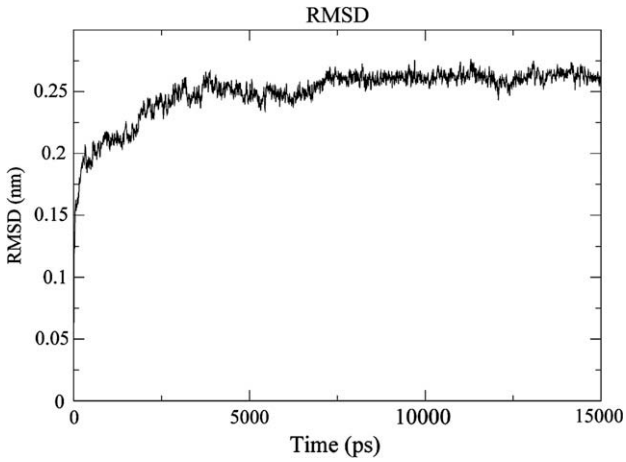

Figure 2. Simulation time versus RMSD of the Cα of the μ opioid receptor.

of EMs and its analogs, and to study the key ligand–receptor interaction involved in the molecular recognition process.

Using the homology modeling method, Mosberg and Fowler[8] have reported a kind of MOR models based on the bovine rhodopsin structure, and we also constructed a homology MOR using the same template.[9] Comparing the two models, it was found that the model built by Mosberg et al. was more suitable for docking peptide agonists, because structural alterations are incorporated into this model to obtain an active state receptor structure (Supplementary data S1). Based on these results, the Mosberg 'active' MOR model was chosen as the working receptor model. The model was then refined using a 15-ns molecular dynamics (MD) simulations in the phospholipid bilayer. The receptor was inserted into a pre-equilibrated 70×70 Å dipalmitoylphosphatidyl-choline (DPPC) bilayer slab (moose.bio.ucalgary.ca), the protein membrane system was embedded in a SPC water box (Supplementary data S2). Counterions were added to the system in order to produce a neutral charge on it. MD simulations were performed with the GROMACS 3.3.3 package employing NPT and periodic boundary conditions.[10] A modification of GROMOS87 force field is applied for protein and the lipid.[11] A twin cutoff of 9 Å was used for the short range interaction and a cutoff of 12 Å was used for the Lennard-Jones interaction. Particle Mesh Ewald (PME) algorithm was used for the calculation of electrostatic contributions to energies and forces.[12] Bond length was constrained using the LINCS algorithm.[13] The systems were coupled to a temperature bath at 300 K, with a coupling constant of 0.1 ps. Semiisotropic coupling with time constant of 1 ps was applied to keep the pressure at 1.0 bar.[14] The system was first energy minimized using the steepest descent integrator for 5000 steps. Then a progression of position restraint was performed for 300 ps. Finally, a 15-ns simulation was performed with a time step of 2 fs. The root mean square deviation was calculated for the backbone atoms of MOR, the receptor became stable after approximately 7.5 ns (Fig. 2). The average structure of the last 1 ns trajectory was considered as the typical structure of the MD simulations.

The molecular dockings were performed with the AUTODOCK4.[15] This program suite uses an automated docking approach that allows ligand flexibility, and it employs Lamarckian Genetic algorithm to treat the ligand–receptor interaction. For all analogs, the NMR conformations were used as starting structures, and the amide group of Tyr1 was protonated. Partial charges, necessary for the docking protocol, were assigned according to the Gasteiger–Marsili scheme. The grid maps representing the opioid receptors in the docking process were calculated with AutoGrid. The docking process was performed in two steps.[16,17] First, a box of $42 \times 42 \times 42$ Å, centred on one of the oxygen atoms of the Asp147, was used with a grid resolution of 0.55 Å. The initial position of the ligand was random. The population size was 100, the maximum number of generations was 27,000, and the maximum number of energy evaluations was 2,500,000. The lowest docking energy conformations or the lowest docking energy conformations included in the largest cluster were considered to be the most stable orientations. In the second step, a box of $40 \times 30 \times 50$ Å, centred on the best conformations obtained in the first step, was used with a resolution of 0.3 Å. The number of energy evaluations was changed to 25,000,000 and the population size was raised to 500. The resulting orientations were scored based on the docking and binding energies and on the distance of Asp147 to the protonated nitrogen of the ligand. The docked energies was calculated using the modified scoring function as reported recently,[18] the correlation between the predicted binding energies and the experimental values was $R = 0.72$ (Supplementary data S3). This value appears to be reasonable considering the high flexibility of our complexes. Experimental studies suggested that the protonated nitrogen moiety interacts with the carboxyl group of Asp147 to form a putative salt bridge and mutated this residue to Ala/Asn or Glu leading to diminished binding affinities. This residue is believed to be the primary binding site.[19]

The obtained docking orientation of **EM1** (Fig. 3a) shows that the binding site is located in the central core of transmembrane helix 3 (TM3), TM5 TM6 and extracellular loop2 (EC2), the Tyr1 lies at the bottom of the binding site and its protonated nitrogen moiety interacts with the carboxyl group of Asp147 (TM3) to form a salt bridge (3.2 Å). The rest of the ligand is orientated towards the extracellular surface. Two hydrogen bonds are formed between the ligand and the receptor: one between the backbone oxygen of Pro2 and the hydroxyl group of Thr218 in EC2, and one between the amide group of the Phe4 and the carboxyl group of Glu229 in EC2. **EM1** is also stabilized by many stacking interactions with the aromatic moieties of the receptor. The side chain of Tyr1 is pointing towards a hydrophobic pocket composed mainly of the aromatic residues Tyr148 (TM3), Phe152 (TM3), Phe237 (TM5) and Trp293 (TM6). The aromatic groups of Trp3 and Phe4 are involved in stacking interactions with the side chains of Phe221 (EC2), Tyr299 (TM6) and Trp318 (TM7). Site-directed mutagenesis experiments have already determined the importance of Asp147, Tyr148, Glu229 and Trp318,[8,20–23] and our proposed model is in good agreement with the available mutation studies. The binding mode of **EM2** (Fig. 3b) is generally the same as that of **EM1**, however, **EM2** shows a lengthened salt bridge in its interaction with Asp147 (3.3 Å).

The results of the molecular docking of the rest compounds adopt very similar conformations and orientations in the binding site. In both ligand **1** and **2** (Fig. 3c and d), the aromatic moieties

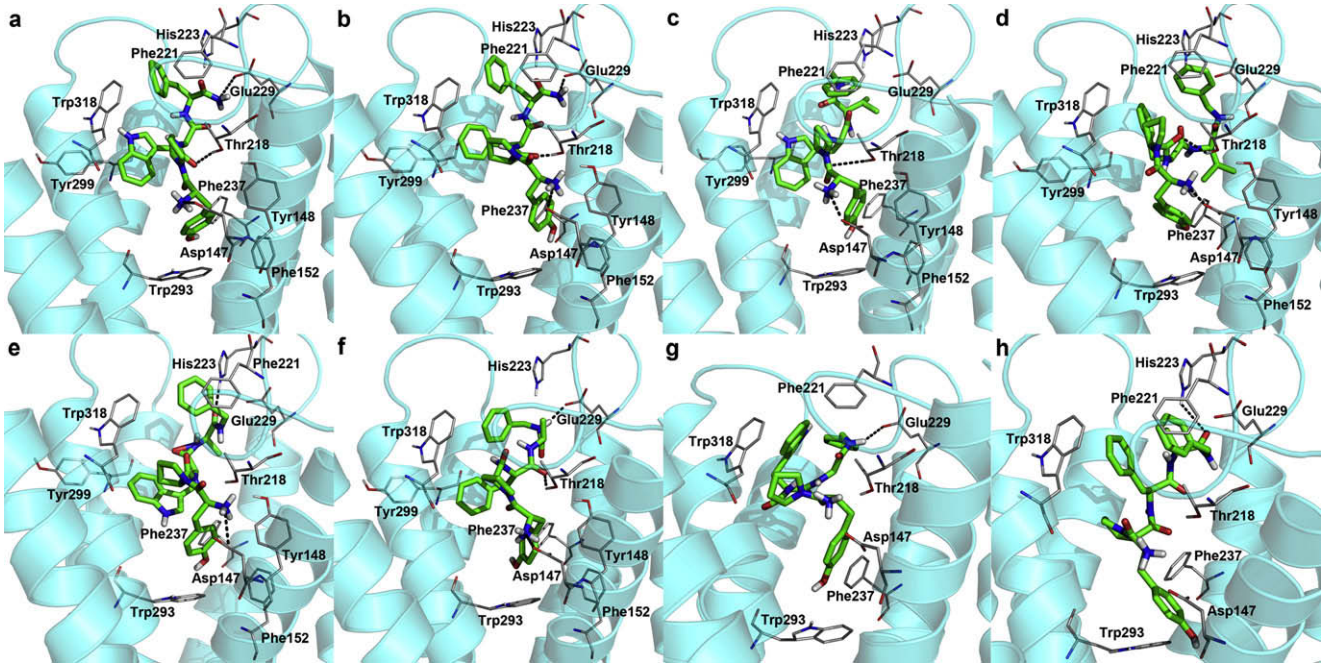

Figure 3. Docked ligand–receptor complexes. (a) **EM1**, (b) **EM2**, (c) ligand **1**, (d) ligand **2**, (e) ligand **3**, (f) ligand **4**, (g) ligand **5**, (h) ligand **6**. Hydrogen bonds are shown as dotted black lines. The ligand, key residues and the receptor are represented as stick, line and cartoon, respectively. Figures are drawn by means of PyMol.[25]

of Tyr1, Trp3 (Phe3 for ligand 2) and benzyl group (the third aromatic ring) are always inserted inside the aromatic clusters as described for **EM1** and **EM2**, and the backbone oxygen of Pro2 forms a hydrogen bond with the hydroxyl group of the Thr218. However, there is no hydrogen bond form between the two ligands and the carboxyl group of Glu229. In ligand **3**, the backbone oxygen of D-Ala4 formed a hydrogen bond with His223 (EC2) (Fig. 3e). In ligand **4**, a hydrogen bond between the backbone oxygen of Phe3 and Thr218 is formed, and the carboxamide moiety of D-Ala4 is hydrogen-bonded to the carboxyl group of Glu229, however, the ligand does not show obvious aromatic interaction with the Phe221 (Fig. 3f). Ligand **5** and **6** show the poorer binding affinities, a result which may be related to an inadequate interaction within the binding site (Fig. 3g and h), the distance between the carboxyl group of Asp147 and the protonated moiety of Tyr1 is 4.6 Å and 4.8 Å, respectively. The aromatic groups of the two ligands are generally inserted in the previously described pockets, but their interactions with Tyr299 are weakened. These structures are also stabilized by hydrogen bonds between carboxyl group of Glu229 and carboxamide moiety of Gly4 for ligand **5** and between His223 and the backbone oxygen of Ala4 for ligand **6**. The residues within 5 Å of each ligand are listed in the Supplementary data S4.

The results obtained from molecular docking of the subject EM analogs allow us to propose a general binding mode of these ligands. The docking models suggest that the interaction between Asp147 (TM3) and Tyr1 could be essential for the ligand binding. In addition, several aromatic residues are involved in ligand binding and may play an important role in stabilizing the ligand orientation.

In the next stage of the study, six molecular dynamics simulations including all the docking models (except ligand **2** and **3**, because of their structure similarities with ligand **1** and **4**, respectively) are performed by using the GROMACS program to get a more reasonable ligand–receptor binding mode, where the flexibility of the receptor was considered. Each ligand–receptor complex was subjected to a 5 ns MD simulation in the previously described membrane bilayer. The topologies of the ligands were generated by PRODRG.[24] The time evolutions of the RMSD of Cα and total energy were analyzed to evaluate the stability of each system. As shown in the Supplementary data S5–6, all systems became stable after about 2 ns MD simulations.

The binding modes of the **EM1** and **EM2** established after MD simulations are nearly the same as that obtained after the molecular docking. However, some additional interactions are formed between the ligands and the receptor: in **EM1**, the protonated nitrogen moiety of Tyr1 is involved in a cation–π interaction with Tyr326 (TM7), which was found to be the key residue for agonist binding by mutagenesis studies.[22] The backbone oxygen of Trp3 loses its contact with Thr218 but forms a hydrogen bond with the side chain of Lys233 (EC2), and a new hydrogen bond is formed between the backbone oxygen of Pro2 and the hydroxyl group of Tyr148 (Fig. 4a). In **EM2**, Tyr148 seems to be involved in π–π interactions with Tyr1 and both the side chain of Tyr148 and Thr218 form a hydrogen bond with the backbone oxygen of Pro2, respectively (Fig. 4b). The differences of the hydrogen bonding modes between **EM1** and **EM2** are possibly due to the conformational flexibility of the two endomorphins. The results of the MD simulations obtained for ligand **1** and **4** suggest that the two D-amino acid substituted ligands experienced similar structural variation during the simulations, the obtained average structures of the two ligands are nearly the same, therefore we mainly take ligand3 into discussion. The most significant variation in ligand3 involves the Trp3 (Phe3 for ligand **4**), which reorients its indole side chain to the bottom of the binding pocket and, as a result, the side chain of Tyr1 moves towards the Trp326 of TM7. The side chains of Tyr1 and Trp3 are then inserted in the same aromatic pocket composed of Tyr148, Phe152, Phe237, Phe241, Trp293 and Trp326. Because of the movement of Trp3, the hydroxyl group of Thr218 is then interacting with the backbone oxygen of D-Val4 through a hydrogen bond (D-Ala4 for ligand **4**). During the MD simulations, two additional hydrogen bonds are formed between the carboxamide of D-Val4 and carboxyl group of Glu229 and between the backbone oxygen of Pro2 and hydroxyl group of Tyr148, respectively, these two kinds of hydrogen bonds are also observed in **EM1**, **EM2** and ligand **4**. Phe221 and Trp318 remain almost unaffected by the binding with the benzyl group, whereas the side chain of Tyr299

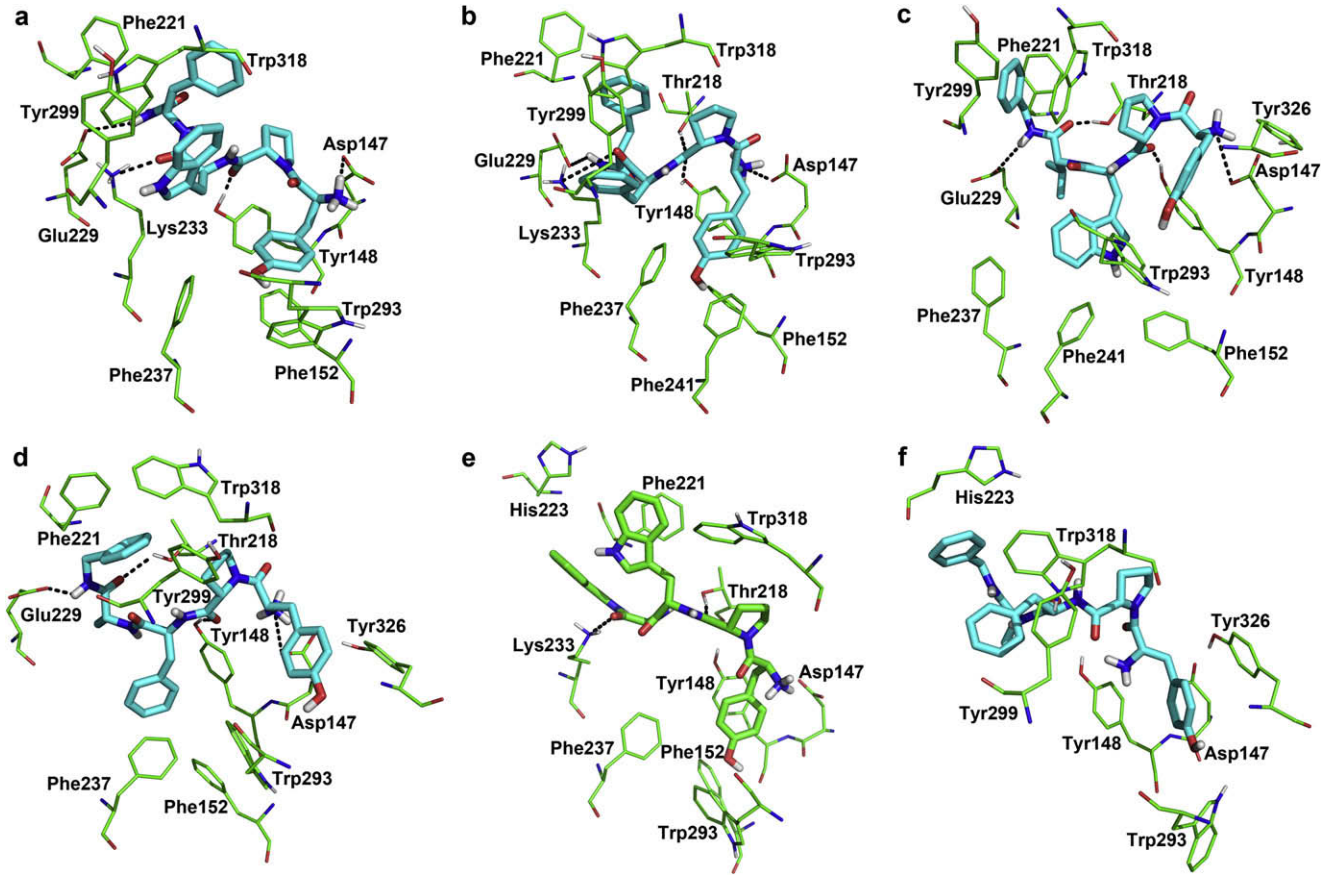

Figure 4. Binding modes of the six ligands obtained after MD simulations. (a) **EM1**, (b) **EM2**, (c) ligand **1**, (d) ligand **4**, (e) ligand **5**, (f) ligand **6**.

loses its contact with the ligand. The analysis of the binding modes of ligand **5** and **6** obtained after MD simulations suggest that the two ligands adopt more 'stretched' geometry with respect to the starting conformation, however, because the two ligands have weak interactions with the receptors in the initial structures, they become 'unstable' during the simulation time, and their interactions with the essential residue Asp147 are still very weak (distance beyond 4.6 Å). For ligand **5**, the hydrogen bond formed between Glu229 and the ligand has broken, however, the hydroxyl group of Thr218 forms a hydrogen bond with the backbone oxygen of Pro2 and the NH3 group of Lys233 moves towards the ligand and forms a hydrogen with the backbone oxygen of Gly4, and for ligand **6**, His223 moves far away from the binding pocket and loses its contact with the ligand, as a results, there is no hydrogen bond found between this ligand and the receptor. The main interactions between the ligands and the receptor obtained from the MD simulations are summarized in the Supplementary data S7.

The analysis of the results of molecular docking and molecular dynamics simulations of the ligand–receptor systems suggests a good agreement between our study and the site-directed mutagenesis data. It is found that Glu229 on EC2 could be essential for the binding of the ligand. It probably 'anchors' the address domain of the ligand at the right position inside the binding pocket, so that the ligand could have close interactions with the receptor. Another important finding is that in the D-amino acid substituted ligands, both the side chains of Trp3 and Tyr1 insert into the aromatic pocket which is composed of the residues located in TM3, 5, 6 and 7, and this different binding mode probably explains the better binding affinities of these ligands. Additionally, Thr218 is predicted to be involved in the hydrophilic interactions with the ligand, and some aromatic residues, in particular Phe152, Phe221, Phe237, Trp293 and Tyr299, could be essential for ligand recognition through π–π interaction.

In summary, the molecular docking procedure was applied to determine the possible positions and orientations for our ligands in the receptor. The MD simulations performed in phospholipid bilayer were then used to optimize the reasonable binding poses of ligand–receptor complex. Some essential amino acids participating in ligand binding were also identified. The elucidation of ligand–receptor interaction would be helpful for the discovery of new active analogs of endomorphin.

Acknowledgements

This work was supported by grants from the National Natural Science Foundation of China (Nos. 90813012, 20621091 and 20525206) and the Chang Jiang Program of the Ministry of Education of China. The authors thank The High Performance Center of Lanzhou University for providing computational resource.

Supplementary data

Supplementary data (the correlation, RMSD and energy plots for the studied complexes and the summary of the residues located within 5 Å of the ligand) associated with this article can be found, in the online version, at doi:10.1016/j.bmcl.2009.07.121.

References and notes

1. Chen, Y.; Mestek, A.; Liu, J.; Yu, L. *Biochem. J.* **1993**, *295*, 625.
2. Waldhoer, M.; Bartlett, S. E.; Whistler, J. L. *Annu. Rev. Biochem.* **2004**, *73*, 953.
3. Zadina, J. E.; Hackler, L.; Ge, L. J.; Kastin, A. J. *Nature* **1997**, *386*, 499.

4. Przewlocki, R.; Labuz, D.; Mika, J.; Przewlocka, B.; Tomboly, C.; Toth, G. *Ann. N.Y. Acad. Sci.* **1999**, *897*, 154.
5. In, Y.; Minoura, K.; Ohishi, H.; Minakata, H.; Kamigauchi, M.; Sugiura, M.; Ishida, T. *J. Pept. Res.* **2001**, *58*, 399.
6. Schwyzer, R. *Ann. N.Y. Acad. Sci.* **1977**, *297*, 3.
7. Yu, Y.; Shao, X.; Cui, Y.; Liu, H. M.; Wang, C. L.; Fan, Y. Z.; Liu, J.; Dong, S. L.; Cui, Y. X.; Wang, R. *ChemMedChem* **2007**, *2*, 309.
8. Mosberg, H. I.; Fowler, C. B. *J. Pept. Res.* **2002**, *60*, 329.
9. Liu, X.; Kai, M.; Jin, L.; Wang, R. *J. Comput. Aided Mol. Des.* **2009**, *23*, 321.
10. Berendsen, H. J.; Vanderspoel, D.; Vandrunen, R. *Comput. Phys. Commun.* **1995**, *91*, 43.
11. Vanbuuren, A. R.; Marrink, S. J.; Berendsen, H. J. C. *J. Phys. Chem.* **1993**, *97*, 9206.
12. Darden, T.; York, D.; Pedersen, L. *J. Chem. Phys.* **1993**, *98*, 10089.
13. Hess, B.; Bekker, H.; Berendsen, H. J. C.; Fraaije, J. *J. Comput. Chem.* **1997**, *18*, 1463.
14. Berendsen, H. J. C.; Postma, J. P. M.; Vangunsteren, W. F.; Dinola, A.; Haak, J. R. *J. Chem. Phys.* **1984**, *81*, 3684.
15. Morris, G. M.; Goodsell, D. S.; Halliday, R. S.; Huey, R.; Hart, W. E.; Belew, R. K.; Olson, A. J. *J. Comput. Chem.* **1998**, *19*, 1639.
16. Hetenyi, C.; van der Spoel, D. *Protein Sci.* **2002**, *11*, 1729.
17. Hetenyi, C.; van der Spoel, D. *FEBS Lett.* **2006**, *580*, 1447.
18. Hetenyi, C.; Paragi, G.; Maran, U.; Timar, Z.; Karelson, M.; Penke, B. *J. Am. Chem. Soc.* **2006**, *128*, 1233.
19. Befort, K.; Tabbara, L.; Bausch, S.; Chavkin, C.; Evans, C.; Kieffer, B. *Mol. Pharmacol.* **1996**, *49*, 216.
20. Li, J. G.; Chen, C.; Yin, J.; Rice, K.; Zhang, Y.; Matecka, D.; de Riel, J. K.; DesJarlais, R. L.; Liu-Chen, L. Y. *Life Sci.* **1999**, *65*, 175.
21. Chen, C.; Yin, J.; Riel, J. K.; DesJarlais, R. L.; Raveglia, L. F.; Zhu, J.; Liu-Chen, L. Y. *J. Biol. Chem.* **1996**, *271*, 21422.
22. Mansour, A.; Taylor, L. P.; Fine, J. L.; Thompson, R. C.; Hoversten, M. T.; Mosberg, H. I.; Watson, S. J.; Akil, H. *J. Neurochem.* **1997**, *68*, 344.
23. Surratt, C. K.; Johnson, P. S.; Moriwaki, A.; Seidleck, B. K.; Blaschak, C. J.; Wang, J. B.; Uhl, G. R. *J. Biol. Chem.* **1994**, *269*, 20548.
24. Schuttelkopf, A. W.; van Aalten, D. M. *Acta Crystallogr., Sect. D* **2004**, *60*, 1355.
25. DeLano, W. L. DeLano Scientific, Palo Alto, CA, USA. 2002.